

pubs.acs.org/JPCC Article

Impact of Photo-induced Physical and Chemical Processes on Lateral Transport of Excitons in Quantum Dot Thin Films

Dustin T. Roberts and Seyed M. Sadeghi*



Cite This: J. Phys. Chem. C 2023, 127, 12143-12151

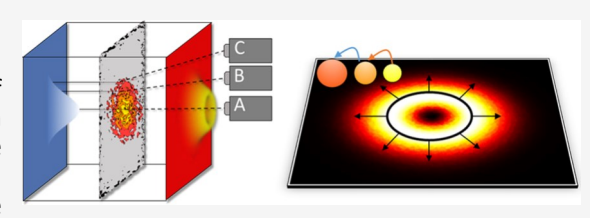


ACCESS

III Metrics & More

Article Recommendations

ABSTRACT: We study how lateral transport of excitons (exciton diffusion) in quantum dot thin films is influenced by the photo-physical and photo-chemical properties of the quantum dots. For this, thin layers of colloidal quantum dots on glass substrates are exposed to laser pulses with different total average powers. Spatial mappings of the lifetimes of the quantum dots within the diffraction-limited spot sizes of the laser beam show that their photo-induced properties can be influenced by the excitation intensity mode profiles significantly, leading to three distinct



regimes of exciton diffusion across the films. These include the cases wherein the lateral energy transport (i) is linearly influenced by the laser intensity mode profiles, (ii) is convoluted by variations of laser intensity and photo-physical and photo-chemical properties of the quantum dots, and (iii) is significantly influenced by the formation of oxidation hole burning. The third regime, oxidation hole burning effect, occurs at the center of the excited regions of the quantum dot thin films, suppressing their emission and transport of energy considerably. We will discuss variations of the diffusivity as a function of the laser intensity mode profiles and time. The results shed light on the impact of photo-chemical and photo-physical processes on transport of energy in quantum dot thin films, highlight the regimes of efficient exciton diffusion, and demonstrate the prominent impact of the intensity mode profiles of the light used to excite quantum dot thin films.

1. INTRODUCTION

Transport of excitation energy without the exchange of carriers or photons is in the front line of ongoing research toward novel optical and energy devices, 1-5 sub-wavelength energy waveguide designs,⁶ and understanding of energy transfer in nanoscale systems and biological materials.7-11 In many semiconductor systems, energy transport is based on the spatial transfer of excitons. Such a process has been studied in different types of systems, including biological systems, 12 transition-metal dichalcogenide monolayers, 13 quantum well structures, 14 and quantum dot (QD) systems. 15-17 Investigation of exciton transport in QD systems is of particular interest as it can occur in three-, two-, and even one-dimensional structures. ^{18,19} As a result, it can have widespread applications, particularly for sensitized solar cells, 10,19-22 quantum computing, 23,24 and quantum dot lasers. 25 QD systems are also interesting for investigation of Fortster resonance energy transfer (FRET), including the control of its rate via plasmonic effects. 26,27-30

Although exciton diffusion and energy transfer in QDs have been studied extensively in the past, ^{31–38} little or no attention has been paid to the impact of excitation intensity on such processes. It is well known that the photoluminescence (PL) of colloidal QDs can be strongly influenced by the wavelength, intensity, and temporal features of the light sources used to optically excite them. ^{39–42} In particular, previous reports have shown that photo-chemical and -physical properties of QDs

can include photo-oxidation, photo-induced fluorescence enhancement, ^{26,43-45} and biexciton auger recombination. ^{44,46} These processes are related to defect generation and passivation by irradiation. ^{44,47} It has further been shown that these processes are dependent on humidity levels. ⁴⁸ It is thought than when QDs are excited well into their conduction bands, the electrons can interact with defects associated with QD surfaces, substrates, and the embedding environments are known to have significant impact on QD devices. ^{3,49} Therefore, a deeper understanding of their development and passivation can shed light on the ongoing research of energy transport in QD-based devices.

In this paper, we study the effects of photo-physical and photo-chemical properties of QDs on exciton diffusion across QD thin films. We demonstrate that such properties impose different regimes of energy transport depending on the intensity of excitation light sources. These include (a) the linear regime, wherein excitation irradiation does not convolute the diffusion process; (b) the moderate regime,

Received: April 6, 2023 Revised: May 24, 2023 Published: June 15, 2023





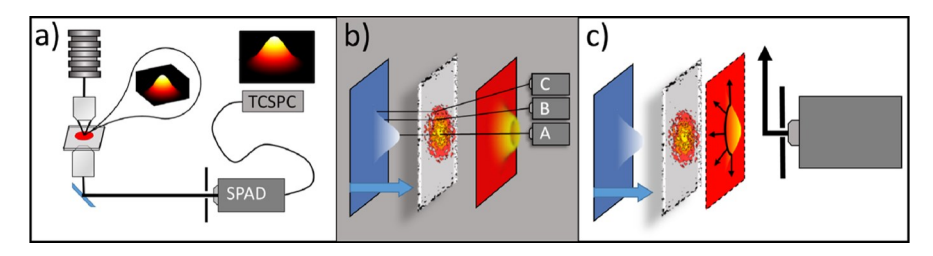


Figure 1. (a) Overall optical setup. An exciton distribution is generated in a QD thin film by exciting it with a diffraction-limited laser spot. (b) TCSPC curves were measured at various positions across the image of the profile formed on the detector/slit combination. The oxidation/enhancement rates at positions A, B, and C across the image of diffraction-limited spot size of the laser beam are measured. (c) Scanning mode of operation used to measure exciton diffusion across the plane of our samples.

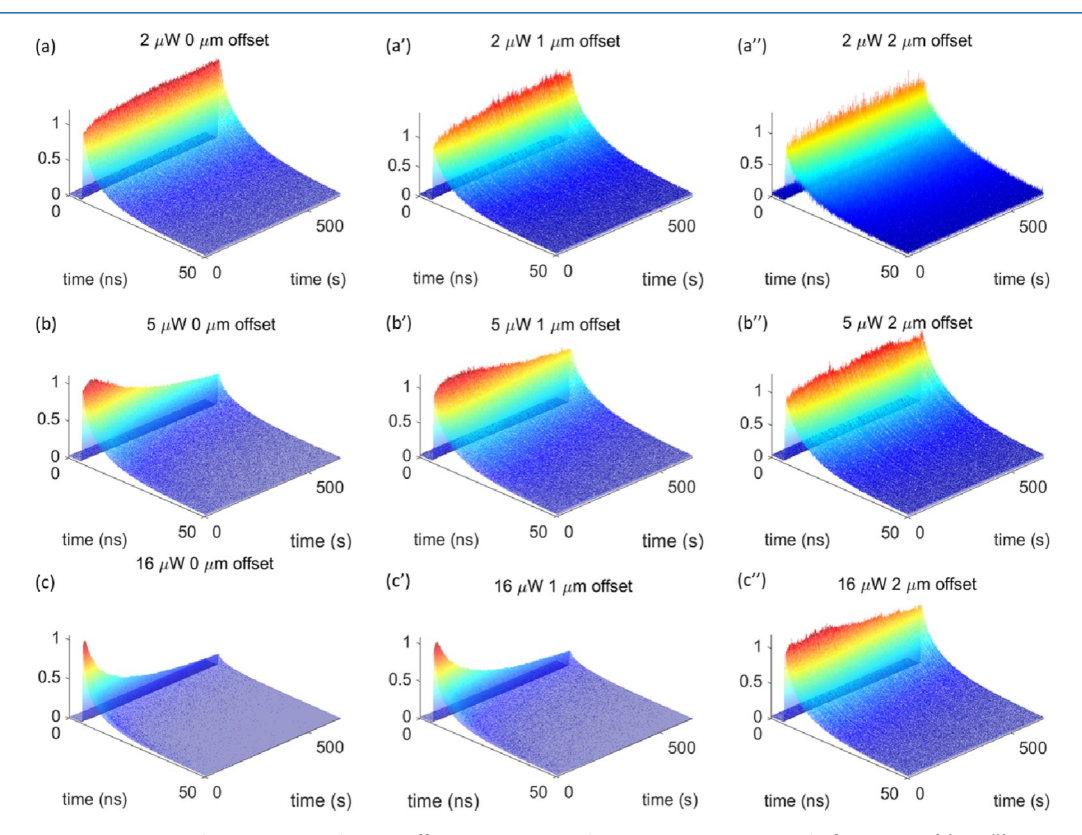


Figure 2. TCSPC curves corresponding to 0, 1, and 2 μ m offsets, i.e., A, B, and C positions in Figure 1b, for TAPs of (a-a") 2 μ W, (b-b") 5 μ W, and (c-c") 16 μ W.

wherein slight oxidation has some impact, yet diffusion is directed from the center of excitation with exciton population toward the outside; and (c) the oxidation hole burning regime, wherein the QDs at the center of excitation spot become dark, causing oxidation hole burning (OHB) such that no energy goes in or out it. In the third regime, exciton diffusion occurs around a ring surrounding the OHB. We study variations of the radiative and non-radiative decay rates associated with these three regimes, highlighting the limiting impact of the excitation profile of the light source used to study exciton diffusion in QDs. Our experimental methodology includes an investigation of the impact caused by various regimes of photooxidation at different positions across the excitation intensity mode profile of the laser beam. The outcomes of this paper are useful for the ongoing research regarding QD device applications and energy transport in QD systems. These include optoelectronics devices such as lasers and detectors^{2,3,5} and QD energy waveguides.⁵⁰

2. METHODOLOGY

QD thin films were fabricated by spin coating a solution of QDs in toluene on glass substrates. The QDs were of the CdSe/Zns core shell type acquired from Ocean Nanotech with a peak emission wavelength of 620 nm. Our experimental setup is shown in Figure 1a. In order to observe the impact of photoinduced processes on PL and QD decay rates, we exposed our samples to a 450 nm-pulsed laser from Picoquant (LDH-P-C-450B) with 30 ps temporal width at a pulse rate of 20 MHz. The laser was focused onto our samples with a full width half maximum (FWHM) of 2 μ m and total average powers (TAPs) ranging from 2 to 32 μ W. This generated an exciton distribution on the sample proportional to the number of photons incident on each position of the excitation profile (Figure 1b). We then projected the image of the resulting PL from these excitons onto the plane of a 20 μm slit placed in front of a single photon avalanche photodiode, which was positioned at various locations across the magnified image. For each combination of laser power and detector position, we

exposed the samples for 657 s while also recording exciton decays using a time correlated single photon counting (TCSPC) system at given time intervals. We normalized these curves to the initial counts, allowing us to observe the change in PL intensity and lifetime over long periods of exposure. Given the FWHM of our excitation area, we decided to probe the photo-induced processes at the center of the excitation profile (position A) and at 1 μ m (position B) and 2 μ m (position C) offsets. In order to ensure the reliability of our data, every measurement was performed with a minimum of three trials. While these measurements allowed us to probe the various regimes of timed photo-induced processes present for each TAP, they did not on their own reveal any information regarding how excitons diffuse on the QD thin films. A key feature of this technique, however, is that it allows us to measure the photo-induced process of QDs at various locations on the excitation profile (Figure 1b) and ultimately study how such a profile influences and convolutes exciton diffusion.

To observe exciton diffusion, we utilized a similar technique to that of Akselrod et al. 38 We excited our samples with a diffraction-limited laser spot at various TAPs. We first pre-exposed our samples for a period of 5 min to allow any photo-induced processes to reach a near steady state, allowing us to ignore ongoing processes during the measurement period. We then continued to expose the sample, scanning our slit and detector across the magnified image of the exciton PL (Figure 1c) and recording TCSPC data at various positions. Our diffusion plots were generated by dividing the TCSPC curves at each position by the TCSPC curve at the position of maximum intensity. Because our system is diffraction-limited, long-lived excitons capable of making multiple transfers are the primary contributors to the broadening of our spatial distribution.

3. IMPACT OF THE IRRADIATION MODE PROFILE ON OXIDATION AND DECAY OF OD THIN FILMS

Figure 2 demonstrates the various regimes of timed photoinduced processes present in different positions (positions A, B. and C as indicated in Figure 1b) of the laser excitation profile. As can be seen from Figure 2a,a", at a TAP of 2 μ W, or 0.25 μ W/ μ m² intensity at the center, the rate of oxidation is insignificant; instead, radiation-induced surface passivation causes some degree of PL enhancement, which stabilizes after several minutes. Since the change in intensity is similar at all three positions, it can be said that the case of 2 μ W falls in a regime wherein the PL-induced enhancement happens with more or less the same rates across the laser beam profile. The PL enhancement seen here can be associated with the surface and field-effect passivation. The latter can be due to the electrostatic field of darkened QDs. This process occurs when photo-excited electrons in a QD are ejected to its defect site, charging the QD. The electrostatic field generated by such a darkened QD suppresses the same process in the neighboring QDs, enhancing their emission. 51-55

Differing degrees of the photo-induced processes become apparent at a 5 μ W TAP. At position A (Figure 2b), we see photo-induced enhancement for the first \$\overline{2}\$100 s of exposure, which can be associated with the surface and field passivation of the defect sites of QDs. \$^{51}\$ A similar passivation has been shown in an appropriately oxygenated environment. \$^{54}\$ In the case of 5 μ W TAP, however, photo-oxidation can generate defects, and the number of the darkened QDs is increased

drastically, leading to a turning point where the PL enhancement is replaced with suppression. Beyond this turning point, the eficiency of the radiative decay of QDs is reduced. In moving to position B (Figure 2b'), we observe a position with lower intensity, and thus a lower rate of defect generation and QD darkening. As a result, the enhancement turning point occurs after a longer time. At position C, the excitation (Figure 2b") intensity is low enough that almost no defects are generated and the scenario seen in Figure 2a-a" is repeated.

To further see the impact of laser excitation power and the beam profile in Figure 2c–c", we show the results for the case of 16 μ W TAP. Once again, the center of the excitation profile shows an initial enhancement, but the degree of PL quenching due to defect sites is far more significant than either of the previous TAPs. The same effect is observed at position B but not at position C. Since we know the intensity as a function of position, we can approximate the threshold at which oxidation begins to occur as approximately 0.7 μ W/ μ m² at our pulse rate, wavelength, and pulse width. We found this approximate threshold by finding the maximum irradiance at which oxidation does not occur over the 500 s time period as seen in Figure 2. Irradiances were calculated as a function of position for a Gaussian distribution with a given TAP and width, as defined by our experimental methods.

Previous reports have shown that the introduction of defect sites reduces the size of the QDs, in turn causing a blueshift in their emission spectra. Figure 3a,b shows spectral variations of the QD emission over time for 2 and 32 $\mu\rm W$ TAPs. In the case of 2 $\mu\rm W$, there seems to be no spectral change. We can also see from Figure 3b that for the case of 32 $\mu\rm W$ TAP, the PL decreases with exposure time at higher powers. Another important aspect of the measurements in Figure 2 is that we can compare the QD PL decay rates before

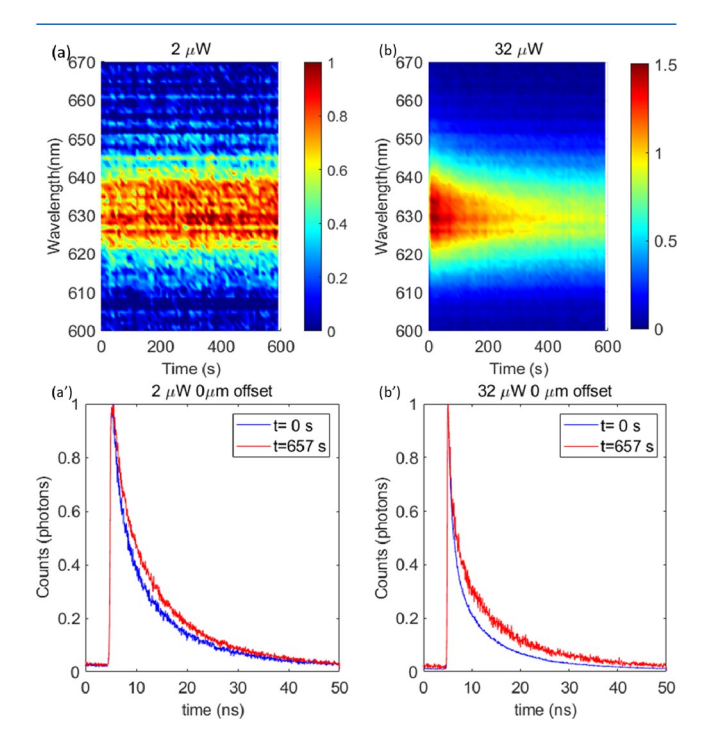


Figure 3. (a, b) QD PL spectra change over time for 2 and 32 μ W, respectively. These spectra are normalized to the maximum value of the initial spectra, allowing us to observe enhancement as well as reduction of emission. (a', b') Normalized decays before and after 600 s of second exposure for 2 and 32 μ W, respectively.

and after the timed exposure period has passed (650 s). From Figure 3a',b', we can see that irradiation decreases the radiative decay rate of the QDs for both 2 and 32 μ W TAPs. These figures also show that the initial decay at 32 μ W TAP in Figure 3b' is much faster than that at 2 μ W TAP in Figure 3a', which indicates the presence of a fast irradiation-dependent decay process. Contrary to our initial expectations, however, this process happens with the elongation of QD lifetime, which is typically a sign of defect passivation.

The results seen in Figure 3 can be explained by considering the fact that low-intensity irradiation can lead to surface passivation, while high intensity can significantly oxidize the QDs. The former can lead to elongation of the QD lifetime, while the latter leads to its shortening in addition to a spectral blueshift. One property of even extreme oxidation is that it is normally reversible over long time scales. To demonstrate the extent of this process in the cases discussed above, we have shown in Figure 4a,b the results of recovery of the QD PL after

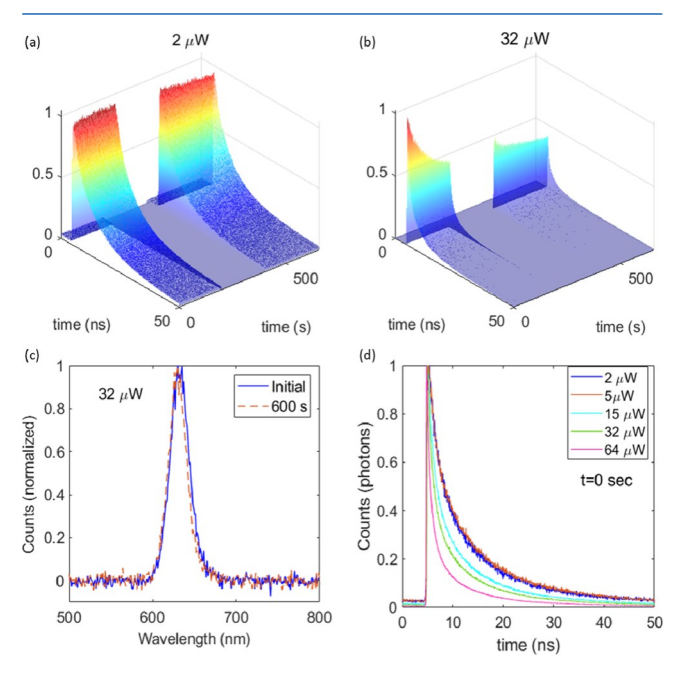


Figure 4. (a, b) Interrupted oxidation measurements taken to observe the possibility of QD recovery after exposure. (c) Normalized PL spectra of QDs before and after 600 s of exposure to 32 μ W TAP. (d) Normalized TCSPC curves at the moment of initial exposure to various TAPs.

a 200 s interruption in the irradiation process for 2 and 32 μ W, respectively. In the case of 2 μ W TAP, we observe that there is no change due to the interruption. For the case of 32 μ W TAP, however, the interruption allows for some recovery of the QD PL. Such a recovery suggests a return of the photo-excited electrons residing in the defect sites back to the QDs.⁵⁵ Lack of extensive oxidation for this can also be seen in Figure 4c, where we compare the normalized line shapes of the QDs at an initial time and after 600 s of irradiation. The results show a minimal amount of blueshift, indicating that while photo-oxidation plays a role, it is not the primary cause of decreased PL. Another important aspect of our measurements is the initial decay rate. Figure 4d demonstrates that the decay rate of excitons at an initial stage of irradiation (t = 0 s) is dependent on the field intensity. As the TAP increases, the decay of QDs becomes faster.

While the results seen in Figure 3a' can be related to photoinduced passivation of QDs, for the case of Figure 3b' one needs to consider the fact that at an early stage of irradiation ($t \approx$ 0 s), the number of photo-induced defect sites is not significant. Therefore, many photo-excited electrons can rapidly undergo transitions to the bottom of the conduction band, forming excitons. As irradiation of the sample proceeds, the density of defects increases. Since the electrons are excited deep into the conduction band, the promotion of electrons into a defect becomes more likely as more defects are formed. As more and more electrons are trapped in defect sites, the number of electrons that undergo intraband transition to the band-edge reduces with exposure. This leads to the reduction of PL intensities seen in Figure 2. Our results suggest that such processes mostly occur for photo-excited electrons in the higher energy portions of the conduction bands of the QDs, while some level of passivation occurs near the band gap.

4. EXCITON DIFFUSION

To investigate diffusion rates in thin films of QDs and the way they are influenced by excitation density, we used the setup in Figure 1c for TAPs ranging from 2 to 32 μ W. These powers are a couple of orders of magnitude larger than those used by other studies,31-38 but they were chosen specifically to highlight the effects of oxidation on diffusion. Figure 5a shows the broadening of the exciton distribution at an incident power of 2 μ W, which serves as a control due to the very small amount of PL intensity and decay changes with exposure. Note that, as shown in Figure 2a–a", a TAP of 2 μW does not significantly modify the PL eficiency; therefore, Figure 5a is comparable with previous studies. 31–38 When excitation power was increased from 2 to 5 μ W (Figure 5b), both the distance and rate of exciton diffusion were increased (i.e., the exciton distribution spreads faster). As power continues to increase to 15 μ W (Figure 5c) and beyond to 32 μ W, another interesting effect of increasing intensity is seen. This effect, referred to here as "oxidation hole burning" or OHB, becomes more pronounced with an increase in TAP (Figure 5d). The probable causes of this process can be the migration of photoexcited electrons to defect sites and formation of defects in the shell or core of the QDs, dangling bonds, and oxide vacancies.^{27,48,56} While reduction in PL intensity is prominent toward the center of the excitation area, as can be seen in Figure 5c,d, there is still an ongoing diffusion process toward the outer edge.

In addition to the broadening seen in Figure 5a-d, we can also use the change in lifetime introduced by diffusion to characterize the diffusive process. In Figure 5a'-d', we have shown the decays of excitons at three positions, each of which is labeled in the corresponding diffusion plot. In order to distinguish between this section and the previous one, we have labeled these positions as positions 1, 2, and 3. For position 1, we have defined consistently at the center of the excitation profile. For TAPs of 2 and 5 μ W, we defined position 2 as a 1 μ m offset and position 3 as a 2 μ m offset. It is easily seen that the lifetime becomes longer with greater distance from the center, following our expected trends (Figure 5a'). As excitons diffuse away from the center, the effective decay rate there should become shorter as excitons occupy that position for a shorter period. Similarly, when they diffuse into a position, the effective lifetime in that position becomes longer. When OHB happens, the oxidation at position 1 introduces another decay pathway, which cannot be distinguished from diffusion. For

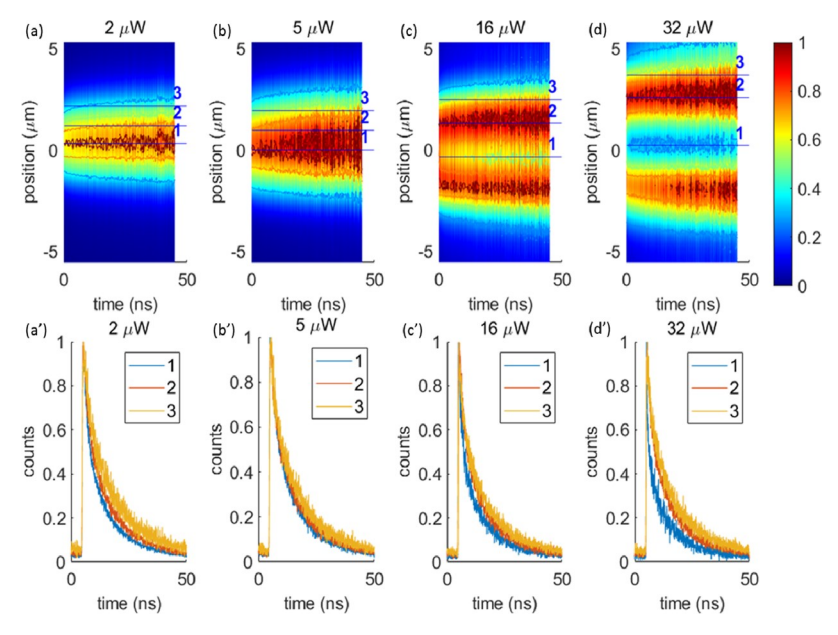


Figure 5. (a-d) Normalized diffusion plots for 2, 5, 16, and 32 μ W TAPs. (a'-d') Normalized decays for positions 1, 2, and 3, as indicated in (a-d).

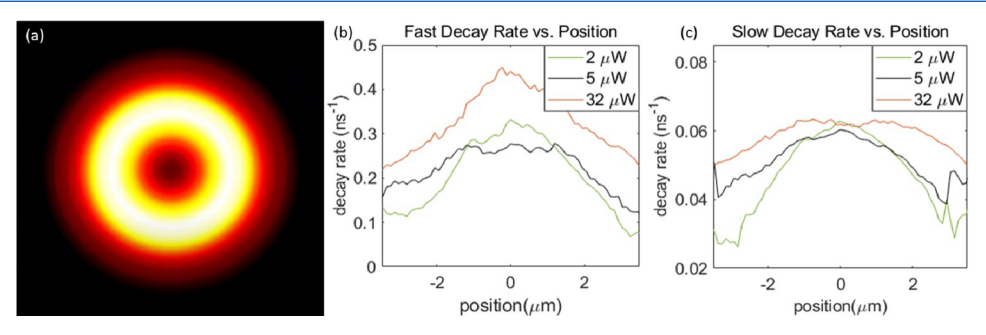


Figure 6. (a) Image of OHB formed by wrapping data from Figure 5c around a center point. (b, c) Fast and slow decay rates found by fitting the raw data used to generate Figure 5 to a biexponential curve.

this reason, we have defined position 2 as the center of the outer ring formed by OHB (Figure 6a) and position 3 as having a 1 μm offset from position 2. In comparing the lifetimes at positions 2 and 3, at TAPs of both 16 μW (Figure 5c') and 32 μW (Figure 5d'), we see that the lifetimes are still longer with increasing distance from the center of the profile. Because of this change in lifetime, we can say that there is diffusion away from the center of the outer ring. As for the center, lack of emission suggests low concentration of exciton population close to the bandgap. The fact that our results do not show diffusion toward OHB indicates a high rate of non-radiative exciton dissociation in this region.

To further analyze the data, we fit our TCSPC curves to a normalized biexponential decay as given below:

$$n = Ae^{-Bt} + CD^{-Dt} (1)$$

In this equation, we have defined B as the fast decay rate associated with non-radiative processes and D as the slower rate associated with radiative processes. A and C represent the amount of contribution from each term. We plotted the resulting fast and slow decay rates as a function of position (Figure 6b,c). For TAPs of 2 and 5 μ W, the non-radiative decay dynamics (i.e., fast decay rates) are relatively similar, but when the TAP is increased to 32 μ W, the non-radiative rate increases significantly. The central peak here indicates the dark

region caused by photo-oxidation. From Figure 6c, we can see that the band-to-band radiative decay process is relatively unaffected by the increase in intensity after the exposure time has passed, which is a further indication of an exposure-related passivation of the initially faster decay process seen in Figure 4d.

Variations of A and C with excitation power provide some further insights into mechanisms responsible for the results seen in Figure 6. We show in Figure 7a,b that the decay

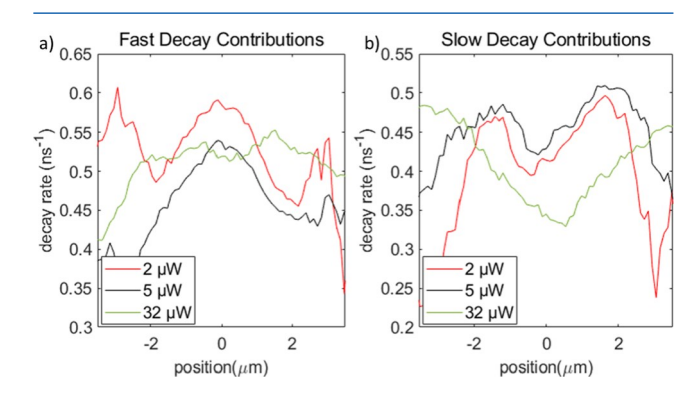


Figure 7. Relative contributions of the (a) non-radiative (i.e., faster) decay processes and (b) radiative (i.e., slower) decay processes.

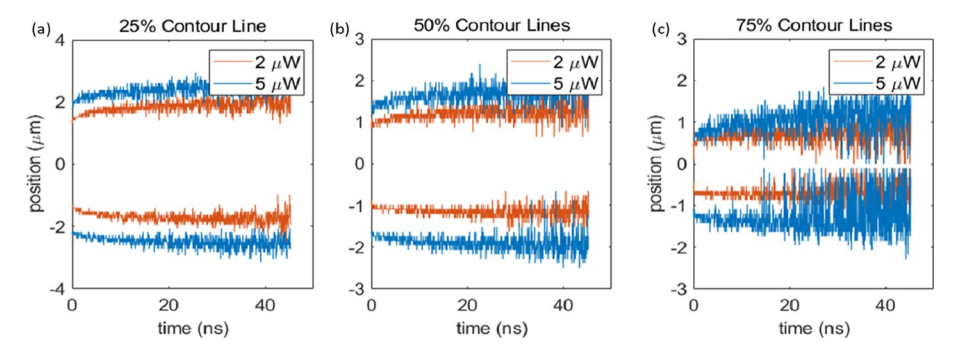


Figure 8. Isolated contour lines from Figure 5a,b at (a) 25%, (b) 50%, and (c) 75% levels.

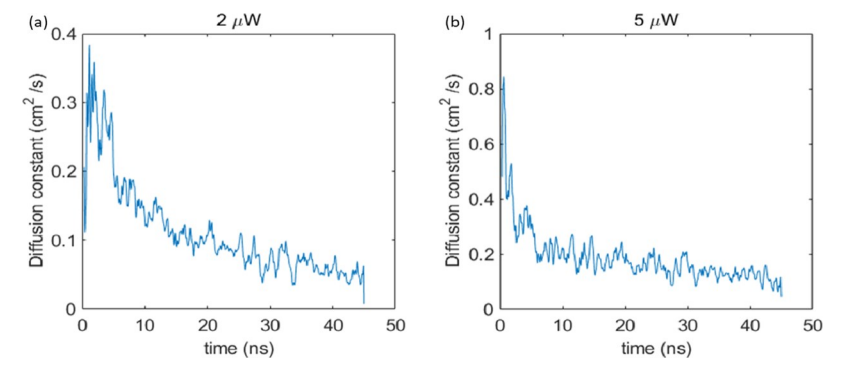


Figure 9. Diffusion constant as a function of time for (a) 2 μ W and (b) 5 μ W TAPs.

processes close to the center of the excitation area are dominated by non-radiative processes, while at the outer parts of the excitation area, radiative recombination dominates. This is especially true for the case of 32 μ W TAP, where the relative contribution of the radiative decay process drops significantly toward the center of the excitation area (Figure 7b). For the case of 2 μ W TAP, wherein normal diffusion happens, however, A is the highest at the center, indicating eficient transport of energy via non-radiative decay, i.e., diffusion, away from the center. This occurs as C reaches a minimum (Figure 7b). At 2 μ m away from the center, A has a dip, while C reaches its maxima, showing how the balance between radiative and non-radiative decay via energy transfer in QDs is influenced by position.

Many diffusive systems, such as those involving heat transfer and fluid displacement, are based upon random walk processes in which the energy does not change between one step and the next. When the diffusion of excitons through a thin film of quantum dots is considered, these steps do not necessarily preserve the energy of the excitons. The widely accepted model of energy transfer between quantum dots is FRET, which is the most eficient when the emission band of the donor overlaps well with the absorption band of the acceptor.³⁸ The net result is that the exciton loses energy with every step along its path, and in some cases, a step is even irreversible. This results in a disordered energy landscape, meaning that sub-diffusive transport is the ideal statistical model to describe exciton diffusion in QD solids and films.⁵⁷ We relate the broadening of our Gaussian to the timedependent diffusivity in eq 2:

$$\sigma^2(t) - \sigma^2(0) = Dt \approx At^{\alpha}$$
 (2)

where σ is the standard deviation, or width, of the Gaussian as a function of time, D is the time-dependent diffusivity, and A and α are parameters describing sub-diffusive transport.

In order to utilize this equation, we first found our variance as a function of time from the FWHM contour shown in Figure 8b. We then found an approximate time-dependent diffusivity by dividing our change in variance by the elapsed time, giving the apparent power relation shown in Figure 9a,b. The results in this figure show that D is highly dependent on intensity, and, therefore, initial exciton population density. Furthermore, our diffusion constant is 3 orders of magnitude larger than that reported by Akselrod et al.³⁸ and two orders of magnitude higher than that reported by Yoon et al.³⁴ The power function time dependence of the diffusion constant is, however, consistent. This is possibly because our intensity is the same orders of magnitude higher, though further studies should be done to explore the possibility of a connection between the rate of diffusion and the incident TAP. It is interesting to note that FRET, the underlying mechanism of diffusion, is independent of intensity, and the diffusive process itself is not. This is likely due to such factors as availabilities of donors and the change in PL lifetime as a function of power seen in Figure 4d.

Application of Gaussian broadening for quantitative analysis of diffusion is only useful when it is considered to be homogeneous and isotropic. Such analysis does not allow for dynamic descriptions, wherein diffusion rates and PL intensity are functions of position. A more general indication of the rate of diffusion is the difference in the effective decay rates between positions with a large exciton population and small exciton populations. Under normal conditions, i.e., low field intensities, the decay rates of excitons toward the center of our Gaussian appear to be faster than rates toward the outer regions. Conversely, one may also say that as excitons diffuse outward, the effective lifetime of excitons in the outer regions

should become longer. While there is more average diffusion for 5 μ W than for 2 μ W, the change in lifetime from position 1 to 3 is less significant for 5 μ W (see Table 1). This is because

Table 1. Table of Various Parameters That Can be Used to Describe Diffusion

laser power	difference in average decay rate (1–3) (ns ⁻¹)	initial variance (um²)	diffusion constant (mean) cm²/s
2 μW	0.13511	20.8	0.1119
5 μW	0.08514	?1	0.1861

the position associated with line 3 for 2 μ W is closer to the turning point of the distribution (i.e., where the second derivative is the highest) so that while the three lines represent the same position for both cases, the two see different amounts of diffusion into the same position.

5. CONCLUSIONS

We studied how photo-induced processes such as photooxidation and the passivation of trap states are essential for understanding exciton diffusion in QD thin films. In particular, for CdSe/ZnS QDs, we highlighted three governing regimes, wherein depending on the excitation intensity, either such processes do play insignificant or moderate roles or they dramatically change the scope of energy transfer. Our results showed that the power distribution of the laser beam can have detrimental impacts on diffusion of excitons, even forming a central region via OHB (oxidation hole burning) that prohibits and convolutes the transport of excitons. These results also highlight the importance of considering the excitation beam profile when observing the diffusion process in thin films of QDs. We have also demonstrated that while using a timeindependent diffusion constant to describe the broadening of a Gaussian is valid, methods utilizing a change in decay rate should be used in more general cases.



AUTHOR INFORMATION

Corresponding Author

Seyed M. Sadeghi – Department of Physics and Astronomy, The University of Alabama in Huntsville, Huntsville, Alabama 35899, United States; orcid.org/0000-0002-5043-5032; Email: seyed.sadeghi@uah.edu

Author

Dustin T. Roberts – Department of Physics and Astronomy, The University of Alabama in Huntsville, Huntsville, Alabama 35899, United States

Complete contact information is available at: https://pubs.acs.org/10.1021/acs.jpcc.3c02308

Notes

The authors declare no competing financial interest.



ACKNOWLEDGMENTS

This research was supported by the US National Science Foundation under grant no. ECCS-1917544.



REFERENCES

(1) Van Riggelen, F.; Hendrickx, N. W.; Lawrie, W. I. L.; Russ, M.; Sammak, A.; Scappucci, G.; Veldhorst, M. A Two-Dimensional Array

- of Single-Hole Quantum Dots. Appl. Phys. Lett. 2021, 118, 044002-044002.
- (2) Ichiyama, R.; Ninkov, Z.; Williams, S. M.; Robinson, R. S.; Bhaskaran, S. Using Quantum-Dots to Enable Deep-UV Sensitivity with Standard Silicon-Based Imaging Detectors. In *Photonic Instrumentation Engineering IV, Proceedings of SPIE OPTO 2017*, San Francisco, California, United States. SPIE. Vol. *10110*. 2017. doi: DOI: 10.1117/12.2256137.
- (3) Chang, R.; Wang, K.; Zhang, Y.; Ma, T.; Tang, J.; Chen, X.-W.; Zhang, B.; Wang, S. Tunable Performance of Quantum Dot-MoS₂ Hybrid Photodetectors via Interface Engineering. *ACS Appl. Mater. Interfaces* 2021, *13*, 59411–59421.
- (4) Yang, L.; Carter, S. G.; Bracker, A. S.; Yakes, M. K.; Kim, M.; Sung, C.; Vora, P. M.; Gammon, D. Optical Spectroscopy of Site-Controlled Quantum Dots in a Schottky Diode. *Appl. Phys. Lett.* 2016, *108*, 233102–233102.
- (5) Oktyabrsky, S.; Tokranov, V.; Yakimov, M.; Sergeev, A. S.; Mitin, V.. Nanoengineered Quantum Dot Medium for Space Optoelectronic Devices. In *Nanophotonics and Macrophotonics for Space Environments VI, Proceedings of SPIE Optical Engineering + Applications 2012*, San Diego, California, United States. SPIE Vol. 8519. 2012. doi: DOI: 10.1117/12.967124.
- (6) Østfeldt, F. T.; González-Ruiz, E. M.; Hauff, N.; Wang, Y.; Wieck, A. D.; Andreas; Schott, R.; Midolo, L.; Sørensen, A.; Uppu, R.; Lodahl, P. On-Demand Source of Dual-Rail Photon Pairs Based on Chiral Interaction in a Nanophotonic Waveguide. *PRX. Quantum.* 2022, *3*, No. 020363.
- (7) Li, K.; Zhong, B.; Liu, B. Quantum Dot-Sized Organic Fluorescent Dots for Long-Term Cell Tracing. *Proc SPIE 9038, Medical Imaging 2014: Biomedical Applications in Molecular, Stuctural, and Functional imaging 2014, 903819, DOI: 10.1117/12.2045456.*
- (8) Vázquez-González, M.; Carrillo-Carrión, C. Analytical Strategies Based on Quantum Dots for Heavy Metal Ions Detection. *SPIE J. Biomed. Opt.* 2014, *19*, 101503–101503.
- (9) Nam, T. W.; Park, Y.; Jung, Y. S.; Park, H. G. Polychromatic Quantum Dot Array to Compose a Community Signal Ensemble for Multiplexed MiRNA Detection. *ACS Nano* 2022, *16*, 11115–11123.
- (10) Optical Properties of ZnS Quantum Dots. Applications in Solar Cells and Biomedicine. *Biointerface Res. Appl. Chem.* 2022, *13*, 158.
- (11) Sengottuvelu, D.; Shaik, A. K.; Mishra, S.; Ahmad, H.; Abbaszadeh, M.; Hammer, N. I.; Kundu, S. Multicolor Nitrogen-Doped Carbon Quantum Dots for Environment-Dependent Emission Tuning. *ACS Omega* 2022, *7*, 27742–27754.
- (12) Tao, M.-J.; Zhang, N.-N.; Wen, P.; Deng, F.-G.; Ai, Q.; Long, G.-L. Coherent and Incoherent Theories for Photosynthetic Energy Transfer. *Sci. Bull.* 2020, *65*, 318–328.
- (13) Kulig, M.; Zipfel, J.; Nagler, P.; Blanter, S.; Schuller, C.; Korn, T.; Paradiso, N.; Glazov, M. M.; Reichman, D. R. *Exciton Diffusion and Halo Effects in Monolayer Semiconductors*. 2018, *120* (20), 207401. doi: DOI: 10.1103/physrevlett.120.207401.
- (14) Vörös, Z.; Balili, R.; Snoke, D. W.; Pfeiffer, L. N.; West, K. W. Long-Distance Diffusion of Excitons in Double Quantum Well Structures. *Phys. Rev. Lett.* 2005, *94*, No. 226401.
- (15) Lubin, G.; Tenne, R.; Can, A.; Antolovic, I. M.; Burri, S.; Karg, S.; Yallapragada, V. J.; Bruschini, C.; Charbon, E.; Oron, D. Heralded Spectroscopy Reveals Exciton–Exciton Correlations in Single Colloidal Quantum Dots. *ACS Nano Lett.* 2021, *21*, 6756–6763.
- (16) Gil, G.; Corni, S.; Delgado, A.; Bertoni, A.; Goldoni, G. Excitation Energy-Transfer in Functionalized Nanoparticles: Going beyond the Forster Approach. *J. Chem. Phys.* 2016, *144*, 074101–074101.
- (17) Jolene Mork, A.; Weidman, M. C.; Prins, F.; Tisdale, W. A. *Magnitude of the Forster Radius in Colloidal Quantum Dot Solids*. 2014, 118 (25), 13920–13928. doi: DOI: 10.1021/jp502123n.
- (18) Reimer, M. E.; Bulgarini, G.; Erik, E.; Dalacu, D.; Poole, P. J.; Zwiller, V. Bright Single-Photon Sources Based on Self-Aligned Quantum Dots in Tapered Nanowire Waveguides. *J. Phys. Chem. C* 2013, DOI: 10.1117/12.2008717.

- (19) Chang, T.-Y.; Kim, H.-S.; Hubbard, W. A.; Azizur-Rahman, K. M.; Jung Jin, J.; Kim, J.-H.; Lee, W.-J.; Huffaker, D. L. InAsP Quantum Dot-Embedded InP Nanowires toward Silicon Photonic Applications. *ACS Appl. Mater. Interfaces* 2022, *14*, 12488–12494.
- (20) Lewinska, G.; Sosna, D.; Kanak, J.; Danel, K. S.; Sanetra, J.; Sahraoui, B.; Marszalek, K. W. The Role of Small Molecules and Quantum Dots Doping on the Morphology of Layers for Potential Applications in Ternary Solar Cells. *Opt. Mater.* 2022, *134*, 113056–113056.
- (21) Giteau, M.; Oteki, Y.; Kitahara, K.; Miyashita, N.; Tamaki, R.; Okada, Y. Resonant Absorption for Multilayer Quantum Well and Quantum Dot Solar Cells. *SPIE J. Photon. Energy* 2022, *12*, No. 022203.
- (22) Sogabe, T.; Shen, Q.; Yamaguchi, K. Recent Progress on Quantum Dot Solar Cells: A Review. *SPIE J. Photon. Energy* 2016, *6*, 040901–040901.
- (23) Ginzel, F.; Burkard, G. Proposal for a Cavity-Induced Measurement of the Exchange Coupling in Quantum Dots. *Phys. Rev. Res.* 2022, *4*, No. 033048.
- (24) Kim, C. W.; Nichol, J. M.; Jordan, A. N.; Franco, I. Analog Quantum Simulation of the Dynamics of Open Quantum Systems with Quantum Dots and Microelectronic Circuits. *PRX Quantum* 2022, *3*, No. 040308.
- (25) Smowton, P.M.; Sandall, I. C.; Mowbray, D. J.; Liu, H.; Hopkinson, M. Maximising the Gain: Optimising the Carrier Distribution in InGaAs Quantum Dot Lasers. In *Physics and Simulation of Optoelectronic Devices XV, Proceedings of Integrated Optoelectronic Devices 2007*, San Jose, California, United States. SPIE. Vol. *6468*. 2007. doi: DOI: 10.1117/12.702733.
- (26) Sadeghi, S.M.; Wing, W. J.; Patty, K.; Campbell, Q. Control of Photoinduced Fluorescence Enhancement of Colloidal Quantum Dots Using Metal Oxides.In *Nanophotonics Materials XII, Proceedings of SPIE Nanoscience + Engineering 2015*, San Diego, California, United States. SPIE. Vol. *9545*. 2015. doi: DOI: 10.1117/12.2188512.
- (27) Steele, J. L.; Ramnarace, C. M.; Farner, W. R. Surface Plasmon Enhanced FRET. In *Optical Sensing, Imaging, and Photon Counting; nanostructured devices and Applications 2017, Proceedings of SPIE Nanoscience + Engineering 2017,* San Diego, California, United States. SPIE. Vol. 10353. 2017. doi: DOI: 10.1117/12.2274218.
- (28) Wei, H. Exciton-Plasmon Coupling of a Single Quantum Dot and a Metal Nanowire. In *Plasmonics II, Proceedings of SPIE/COS Photonics Asia 2016*, Beijing, China. SPIE Vol. *10028*. 2016. doi: DOI: 10.1117/12.2246216.
- (29) Higgins, L. J.; Zhang, X. Y.; Marocico, C. A.; Murphy, G. P.; Karanikolas, V. K.; Gunko, Y. K.; Lesnyak, V.; Gaponik, N.; Susha, A. S.; et al., A. P. Enhancing Forster Nonradiative Energy Transfer via Plasmon Interaction. In *Nanophotonics VI, Proceedings of SPIE Photonics Europe 2016*, Brussels, Belgium. SPIE Vol. *9884*. 2016. doi: DOI: 10.1117/12.2229032.
- (30) Regler, A.; Schraml, K.; Lyamkina, A. A.; Spiegl, M.; Muller, K. W.; Vuckovic, J.; Finley, J. J.; Kaniber, M. Emission Redistribution from a Quantum Dot-Bowtie Nanoantenna. *SPIE J. Nanophoton.* 2016, *10*, 033509–033509.
- (31) Kholmicheva, N.; Moroz, P.; Bastola, E.; Razgoniaeva, N.; Bocanegra, J.; Shaughnessy, M.; Porach, Z.; Khon, D.; Zamkov, M. Mapping the Exciton Diffusion in Semiconductor Nanocrystal Solids. *ACS Nano* 2015, *9*, 2926–2937.
- (32) Kagan, C. R.; Murray, C. B.; Bawendi, M. G. Long-Range Resonance Transfer of Electronic Excitations in Close-Packed CdSe Quantum-Dot Solids. *Phys. Rev. B* 1996, *54*, 8633–8643.
- (33) Kagan, C. R.; Murray, C. B.; Nirmal, M.; Bawendi, M. G. Electronic Energy Transfer in CdSe Quantum Dot Solids. *Phys. Rev. Lett.* 1996, *76*, 1517–1520.
- (34) Joon, S.; Guo, Z.; Cecilia, P.; Shevchenko, E. V.; Huang, L. Direct Imaging of Long-Range Exciton Transport in Quantum Dot Superlattices by Ultrafast Microscopy. *ACS Nano* 2016, *10*, 7208–7215.
- (35) Lunt, R. R.; Giebink, N. C.; Belak, A. A.; Benziger, J. B.; Forrest, S. R. Exciton Diffusion Lengths of Organic Semiconductor

- Thin Films Measured by Spectrally Resolved Photoluminescence Quenching. *J. Appl. Phys.* 2009, *105*, 053711–053711.
- (36) Ginsberg, N. S.; Tisdale, W. A. Spatially Resolved Photogenerated Exciton and Charge Transport in Emerging Semiconductors. *Annu. Rev. Phys. Chem.* 2020, *71*, 1–30.
- (37) Zhitomirsky, D.; Voznyy, O.; Hoogland, S.; Sargent, E. H. Measuring Charge Carrier Diffusion in Coupled Colloidal Quantum Dot Solids. *ACS Nano* 2013, *7*, 5282–5290.
- (38) Akselrod, G. M.; Prins, F.; Poulikakos, L. V.; Lee, E. M. Y.; Weidman, M. C.; Mork, A. J.; Willard, A. P.; Bulovic, V.; Tisdale, W. A. Subdiffusive Exciton Transport in Quantum Dot Solids. *Nano Lett.* 2014, *14*, 3556–3562.
- (39) Uematsu, T.; Maenosono, S.; Yamaguchi, Y. Photoinduced Fluorescence Enhancement in Mono- and Multilayer Films of CdSe/ZnS Quantum Dots: Dependence on Intensity and Wavelength of Excitation Light. *J. Phys. Chem. B.* 2005, *109*, 8613–8618.
- (40) Uematsu, T.; Maenosono, S.; Yamaguchi, Y. Photoinduced Fluorescence Enhancement in CdSe/ZnS Quantum Dot Monolayers: Influence of Substrate. *Appl. Phys. Lett.* 2006, *89*, 031910–031910.
- (41) Icardo, M. C.; Calatayud, J. M. Photo-Induced Luminescence. *Crit. Rev. Anal. Chem.* 2008, *38*, 118–130.
- (42) Liu, H.; Dong, Q.; Lopez, R. The Effect of Light Intensity, Temperature, and Oxygen Pressure on the Photo-Oxidation Rate of Bare PbS Quantum Dots. *Nanomaterials* 2018, *8*, 341–341.
- (43) Liu, L.; Peng, Q.; Li, Y. An Effective Oxidation Route to Blue Emission CdSe Quantum Dots. *Inorg. Chem.* 2008, 47, 3182–3187.
- (44) Klimov, V. I.; McBranch, D. W.; Leatherdale, C. A.; Bawendi, M. G. Electron and Hole Relaxation Pathways in Semiconductor Quantum Dots. *Phys. Rev. B* 1999, *60*, 13740–13749.
- (45) Ito, Y.; Matsuda, K.; Kanemitsu, Y. Mechanism of Photoluminescence Enhancement in Single Semiconductor Nanocrystals on Metal Surfaces. *Phys. Rev. B* 2007, *75*, No. 033309.
- (46) Klimov, V. I.; McBranch, D. W. Femtosecond1P-To-1SElectron Relaxation in Strongly Confined Semiconductor Nanocrystals. *Phys. Rev. Lett.* 1998, *80*, 4028–4031.
- (47) Schroeter, D. F.; Griffiths, D. J.; Sercel, P. C. Defect-Assisted Relaxation in Quantum Dots at Low Temperature. *Phys. Rev. B* 1996, 54, 1486–1489.
- (48) Pechstedt, K.; Whittle, T.; Baumberg, J. J.; Melvin, T. Photoluminescence of Colloidal CdSe/ZnS Quantum Dots: The Critical Effect of Water Molecules. *J. Phys. Chem. C* 2010, *114*, 12069–12077.
- (49) Hamada, M.; Takenokoshi, N.; Matozaki, K.; Feng, Q.; Murase, N.; Wakida, S.; Nakanishi, S.; Biju, V. In Situ Photochemical Surface Passivation of CdSe/ZnS Quantum Dots for Quantitative Light Emission and Enhanced Photocurrent Response in Solar Cells. *J. Phys. Chem. C* 2014, *118*, 2178–2186.
- (50) Mao, C.; Flynn, C.; Hayhurst, A.; Sweeney, R. Y.; Qi, J.; Georgiou, G.; Iverson, B. L.; Belcher, A. M. Viral Assembly of Oriented Quantum Dot Nanowires. *Proc. Natl. Acad. Sci.* 2003, *100*, 6946–6951.
- (51) Kimura, J.; Uematsu, T.; Maenosono, S.; Yamaguchi, Y. Photoinduced Fluorescence Enhancement in CdSe/ZnS Quantum Dot Submonolayers Sandwiched between Insulating Layers: Influence of Dot Proximity. *J. Phys. Chem. B.* 2004, *108*, 13258–13264.
- (52) Sadeghi, S. M.; Wing, W. J.; Gutha, R. R.; Goul, R.; Wu, J. Z. Functional Metal-Oxide Plasmonic Metastructures: Ultrabright Semiconductor Quantum Dots with Polarized Spontaneous Emission and Suppressed Auger Recombination. *Phys. Rev. Appl.* 2019, *11*, No. 024045.
- (53) Yang, S.; Feng, H.-Y.; Lin, Y.-S.; Chen, W.-C.; Kuo, Y.; Yang, C.-C. Effects of Surface Plasmon Coupling on the Color Conversion of an InGaN/GaN Quantum-Well Structure into Colloidal Quantum Dots Inserted into a Nearby Porous Structure. *Nanomaterials* 2023, 13, 328.
- (54) Zhuang Qi, H.; Liu, S.; Qin, H.; Zhou, J.; Peng, X. Oxygen Stabilizes Photoluminescence of CdSe/CdS Core/Shell Quantum Dots via Deionization. *J. Am. Chem. Soc.* 2020, *142*, 4254–4264.

- (55) Patty, K.; Sadeghi, S. M.; Campbell, Q.; Hamilton, N.; West, R.; Mao, C. Probing the Structural Dependency of Photoinduced Properties of Colloidal Quantum Dots Using Metal-Oxide Photo-Active Substrates. *J. Appl. Phys.* 2014, *116*, 114301–114301.
- (56) Sadeghi, S. M.; Gutha, R. R.; Mao, C. Plasmonic Hot-Electron-Induced Control of Emission Intensity and Dynamics of Visible and Infrared Semiconductor Quantum Dots. *Adv. Mater. Interfaces* 2020, 7, 1901998–1901998.
- (57) Bouchaud, J. P.; Georges, A. Anomalous Diffusion in Disordered Media: Statistical Mechanisms, Models and Physical Applications. *Phys. Rep.* 1990, *195*, 127–293.